Impact of river runoff into the ocean on Indian summer monsoon

2015 Environ. Res. Lett. 10 054008

(http://iopscience.iop.org/1748-9326/10/5/054008)

Environmental Research Letters

LETTER

Impact of river runoff into the ocean on Indian summer monsoon

P N Vinayachandran[1,2], S Jahfer[1] and R S Nanjundiah[1,2]

[1] Centre for Atmospheric and Oceanic Sciences, Indian Institute of Science, Bangalore 560 012, India
[2] Divecha Center for Climate Change, Indian Institute of Science, Bangalore 560 012, India

E-mail: vinay@caos.iisc.ernet.in

Keywords: Monsoon, river runoff, ocean salinty, coupled model, El Niño

OPEN ACCESS

RECEIVED
25 November 2014

REVISED
9 April 2015

ACCEPTED FOR PUBLICATION
20 April 2015

PUBLISHED
11 May 2015

Abstract

Rivers of the world discharge about 36000 km^3 of freshwater into the ocean every year. To investigate the impact of river discharge on climate, we have carried out two 100 year simulations using the Community Climate System Model (CCSM3), one including the river runoff into the ocean and the other excluding it. When the river discharge is shut off, global average sea surface temperature (SST) rises by about 0.5°C and the Indian Summer Monsoon Rainfall (ISMR) increases by about 10% of the seasonal total with large increase in the eastern Bay of Bengal and along the west coast of India. In addition, the frequency of occurrence of La Niña-like cooling events in the equatorial Pacific increases and the correlation between ISMR and Pacific SST anomalies become stronger. The teleconnection between the SST anomalies in the Pacific and monsoon is effected via upper tropospheric meridional temperature gradient and the North African–Asian Jet axis.

1. Introduction

Changes in salinity caused by variations in freshwater input into the ocean can induce changes in ocean circulation and heat transfer (Lagerloef 2002, Seidov and Haupt 2003, Fedorov *et al* 2004). In addition, salinity anomalies can alter sea surface temperature (SST) through its effect on mixed layer dynamics by controlling stratification (Lukas and Lindstorm 1991, de Boyer Montegut *et al* 2007). The resultant SST anomalies would influence the air–sea interaction, wind stress, heat and freshwater fluxes and hence the gyre circulation in a complex nonlinear way. Salinity anomalies induced by freshening of higher latitudes lead to shoaling of the mixed layer and amplification of warming by trapping more CO_2-induced heat in the surface ocean (Zhang and Wu 2012). However, the global mean SST increase caused by doubling of CO_2 is reduced by 10% in a hypersaline ocean (Williams *et al* 2010), implying an intriguing role of freshwater changes on the global SST pattern. Considering that due to anthropogenic activities hydrological cycle is projected to amplify, with wet regions getting wetter and dry regions getting drier (Seager *et al* 2010) and ocean salinity showing corresponding changes (Durack *et al* 2012), it is essential to understand the role of individual components of the hydrological cycle on climate.

The world oceans receive about 36000 km^3 of freshwater annually in the form of river discharge (Dai *et al* 2009, Milliman and Farnsworth 2011). Freshwater input into the oceans by way of runoff is about 10% of the total which falls as precipitation over oceans (Trenberth *et al* 2007). Unlike rainfall, the river runoff is concentrated surrounding the mouths of major rivers initially, and is advected, mixing with the ambient sea water on its way, to distances far away by ocean currents. Consequently, the impact of river runoff is felt over all basins of the world's oceans, even at regions far away from the river mouth. For example, in their numerical experiment using an ocean general circulation model (OGCM), Huang and Mehta (2010) found that blocking of Amazon river discharge into the Atlantic Ocean affects upper ocean temperature in the Indian and Pacific oceans. The role of river discharge in present day climate is, however, not well understood. Seo *et al* (2009) used a regional coupled model (which treated river discharge by salinity relaxation to climatology) to study the effect of runoff into the Indian Ocean on precipitation. They found that the northeast (winter) monsoon rainfall is affected significantly by river discharge through its effect on barrier layer thickness and consequently on SST. To

the best of our knowledge, no study has been carried out using a fully coupled global model to investigate the role of ocean–atmosphere feedback resulting from the river runoff into the ocean. In this paper, using a fully coupled global climate model, we show that river runoff affects the two most important modes of tropical climate; namely El Niño Southern Oscillation (ENSO) and monsoon. A brief description of the model and experiments are presented in the next section. The impact of blocking rivers into oceans, monsoon and El Niño are described in section 3. We wrap up with a brief discussion and conclusions in section 4.

2. Model and Experiments

The model used in this study is the Community Climate System Model Version 3 (CCSM3) (Collins *et al.*, 2006a) which consists of the Community Atmospheric Model (CAM3) (Collins *et al* 2006), Parallel Ocean Program (POP) (Smith and Gent 2002), Community Land Model (CLM3) (Dickinson *et al* 2006), and Community Sea–Ice Model (CSIM5) (Briegleb *et al* 2004). Runoff in the model is parameterized using a variable area contributing model (Beven and Kirkby 1979) and a river transport algorithm (Branstetter 2001) embedded within. The atmospheric model and land model were run at T42 resolution. CAM3 had 26 levels in the vertical and CLM3 had 10 subsurface soil layers. The longitudinal resolution of the ocean model is approximately one degree whereas the latitudinal resolution is 0.27° at the equator, decreasing to 0.54° at 33° latitude and remains at this value towards the poles. There are 40 vertical levels in the ocean model of which 9 are in the upper 100 m. The ocean and ice models have the same horizontal resolution. Initial conditions for the coupled model experiments presented in this paper were obtained from the control run carried out at the National Center for Atmospheric Research (NCAR) with CO_2 concentrations of pre-industrial times and an annual average CO_2 mixing ratio of 355 ppmv (Collins *et al.*, 2006a). The input data for the year 648 was used to restart the model and a 100 year run was carried out, which we refer to in this paper as the control run (CR). The no river runoff run (NoRiv) was started from the same initial condition and run for 100 years by multiplying the river runoff into the ocean by zero. The direct effect of this modification is on the salinity equation.

3. Results

3.1. Impact on oceans

Sea surface salinity (SSS): The primary impact of blocking of global continental discharge into the ocean (figure 1a) is an increase in mean SSS in all major oceans (figure 1(b)). This increase is rapid in the first 30 years and reduces as the simulation progresses. SSS averages

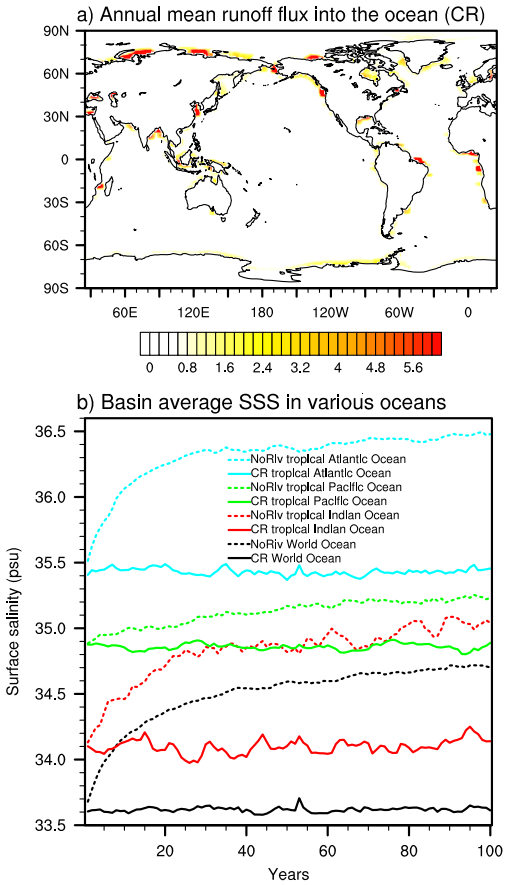

Figure 1. (a) Annual mean global runoff (kg m^2 s^{-1}) into the ocean as simulated in the control run. Red spots are the mouths of major rivers including the Amazon, Congo, Orinoco, Ganges–Brahmaputra etc. (b) Time series of annual mean SSS (psu) from CR (thick line) and NoRiv (dashed line) averaged over the World Ocean (black), tropical (30°S to 30°N) Indian Ocean (red), tropical Pacific Ocean (green) and tropical Atlantic Ocean (cyan). The difference in SSS between NoRiv and CR shows the relative importance of river runoff in various ocean basins. For example, the slower rate of salinity increase in the tropical Pacific is due to the relatively larger size of the basin and less runoff, whereas runoff is important to maintain salinity fields in the Atlantic basin. The rate of salinity build-up in the NoRiv dampened and reached a new quasi–stabilized state after about 50 years of the model run.

over the world ocean increased by about 0.60 psu in the first 15 years, and by 0.12 psu over 30 to 50 years. The model SSS variations attained a nearly steady state after about 50 years. The increase in SSS average over the world oceans in the first 50 years is 0.91 psu, and is 0.11 psu in the last 50 years. In the case of tropical oceans, the SSS increase occurs at a slower pace. When the SSS of the Indian Ocean increased by 0.69 psu in the first 50 years and by 0.21 psu in the last 50 years, the corresponding changes in the Pacific Ocean were 0.29 psu and 0.07 psu, respectively. The tropical Atlantic Ocean, where the effect of the Amazon and Congo rivers is prominent, showed an increase of 0.87 psu in the first 50 years compared to 0.11 psu in the last 50 years. The above quantitative inspection suggests that the rate of change in SSS in the NoRiv reached a quasi–stabilized state in the 50 to 100 year time period

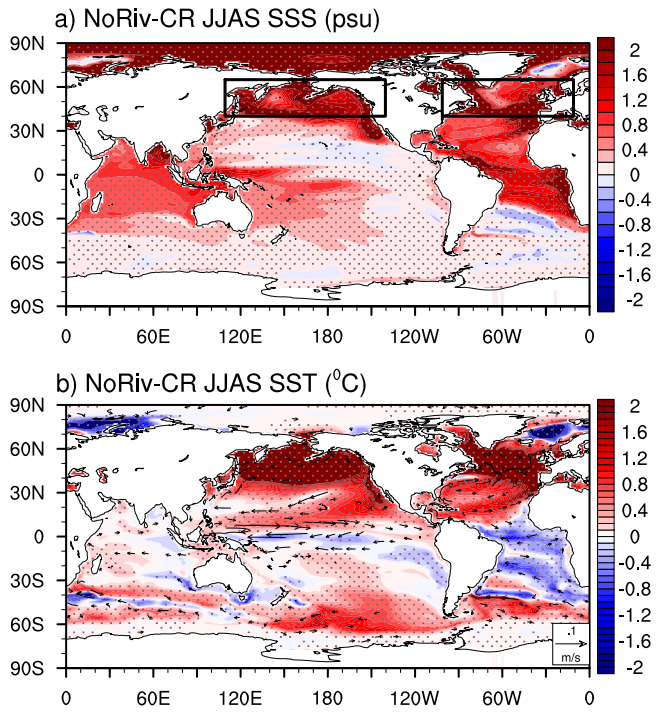

Figure 2. Response of sea surface salinity and temperature to the absence of river runoff. Maps of mean difference of simulations without and with river runoff (NoRiv–CR) averaged for the summer monsoon months of June, July, August and September (JJAS) during the 50–100 year of the model run are shown. (a) Sea surface salinity (psu), (b) sea surface temperature (°C). The differences are significant at 95% confidence level in the stippled region. Vectors in panel (b) are differences (NoRiv–CR) in annual mean currents (m s^{-1}) that are larger than 2 cm s^{-1}. Boxes over the North Atlantic (40°N–65°N, 100°W–10°W) and Pacific (40°N–65°N, 110°E–140° W) in panel (a) enclose the regions of large SSS and SST response in NoRiv.

(figure 1(b)). Therefore, for the convenience of analysis, we have divided the entire model period into two: 1) 1 to 50 years, the perturbation period and, 2) 50 to 100 years, the quasi–stabilized period.

The increase in SSS is initially confined to oceanic regions close to the mouths of rivers but advected away subsequently (figure 2(a)), depending on the pattern and strength of ocean currents and mixing with the surrounding water. The maximum change in the summertime SSS (~3–4 psu), due to the blocking of river discharge, taken as a mean for the last 50 years of model runs, is seen in the Arctic Ocean, owing to the large river discharge into this region (Dai and Trenberth 2002). The effect of the Amazon and Congo rivers is seen in the tropical western and eastern Atlantic, respectively. The anomalies near the Amazon river mouth seem to be lower compared to those near the Congo river mouth, even though the Amazon runoff is considerably higher, due to the presence of strong western boundary currents and stronger mixing. In the tropical Pacific, the mean SSS increase is only 0.3 psu, largely in the western half (0.5 psu), mainly due to the effect of southeast Asian rivers. In the Indian Ocean, the plugging of several rivers discharging into the Bay of Bengal causes a basin-wide increase in salinity (Vinayachandran and Nanjundiah 2009). In the absence of runoff, the surface water turns saltier in the entire tropical Indian Ocean (about 0.8 psu). Salinity anomalies (>3 psu) near the mouths of major rivers in the Bay of Bengal are distributed by boundary currents and inter-basin exchange between the Arabian Sea and Bay of Bengal (Shankar *et al* 2002, Rao and Sivakumar 2003, Vinayachandran and Nanjundiah 2009), leading to a saltier Indian Ocean. On the whole, the response of the salinity in the tropical Atlantic to the freshwater perturbation from rivers (~1 psu increase) is higher compared to the Indian and Pacific Oceans.

In the northern extratropical oceans, high SSS anomalies are seen to occupy a large area and they reach up to the tropics along the eastern boundaries. In order to understand the major processes leading to higher salinities in the northern Atlantic and Pacific oceans in the NoRiv run, we have examined various processes contributing to the salinity tendency within the mixed layer. In order to make the analysis relatively simple, two boxes enclosing the positive SSS difference (shown in figure 2(a)) are considered; one for the northern Atlantic (40°N-65°N, 100°W–10°W) and the other for the northern Pacific (40°N-65°N, 110°E–140°W). An estimate of the freshwater budget in these boxes for both CR and NoRiv has been carried out. Then the difference of dominant terms, namely, (1) P-E (precipitation minus evaporation), (2) net oceanic transport of freshwater into this box and (3) local runoff were examined.

Figure 3(a) shows processes contributing to the increase in salinity in the NoRiv case in the northern Atlantic. Anomalous northward transport of saltier tropical surface waters (leading to an annual mean loss

Figure 3. Mechanism of SSS and SST changes in the Atlantic (left panels) and Pacific (right panels) boxes shown in figure 2(a). 3 year running average of annual mean difference (NoRiv–CR) of freshwater budget terms in the (a) Atlantic and (b) Pacific boxes. The net effect of all freshwater terms in (a) and (b) is shown by the black dashed line. A negative value in (a) and (b) corresponds to a loss of freshwater from the NoRiv ocean compared to CR. The mechanism of warming in the Pacific and Atlantic boxes for the CR (blue) and NoRiv (red) simulations are illustrated in panels c to f. Annual mean net flux at the surface (c, d) and the net mixed layer heat transport into the boxes (e, f) are shown.

of 0.20 Sv of freshwater) as well as a lack of runoff in the NoRiv run (0.18 Sv) largely contributes to the salinity increase. Freshwater loss in the form of P-E (0.12 Sv) also results in salinity build-up. A similar rise in the northern Atlantic SSS was noticed by Huang and Mehta (2010) when Amazon runoff was blocked in an ocean model. They attributed this increase in salinity to the transport of saltier water from low latitudes, mainly due to the strengthening of the Gulf Stream (figure 2(b)), which is consistent with our analysis.

It is clear from figure 3(b) that the major factor that leads to salinity increase in the Pacific is the lack of freshwater supply through river runoff (0.33 Sv). Note that the river runoff into the Pacific box is almost twice that into the Atlantic Box, consistent with the data presented by Dai and Trenberth (2002). The contribution from freshwater loss via P-E is only a third of the river runoff (0.12 Sv in the last 50 years) and that from net meridional freshwater transport (0.015 Sv in the last 50 years) is less by an order of magnitude. The net contribution from these terms results in an annual mean loss of 0.2 Sv of freshwater in the last 50 years.

Sea surface temperature: Blocking of runoff leads to warmer SST in the northern hemisphere tropics and cooling along the equator (figure 2(b)). Maximum warming (about 2.8°C) is seen between 40°–65°N in the Atlantic and Pacific Oceans and maximum cooling (about 2.5°C) in the Arctic Ocean (figure 2(b)). In the northern tropics, warming in the Atlantic is highest (about 1°C) and decreases westward. A similar pattern is also seen in the Pacific. There is weak (less than 0.3°C) warming in the western part of the Indian Ocean and weak cooling in the east that is weaker compared to the Pacific and Atlantic. Clearly, the impact of river discharge can be felt quite far away from the locations of river discharge consistent with the findings by Huang and Mehta (2010) using an OGCM.

The changes in SST are either due to an indirect effect of salinity increase (which is primarily weakening of the stratification in the upper layer) or due to changes in the air–sea heat flux in a coupled system. To determine the primary factors causing the SST difference, we have carried out an analysis of the mixed layer heat budget for the boxes shown in figure 2(a) where the SST anomalies are high. Significant difference between the two runs were found to be in the net surface heat flux and meridional heat transport, and these are presented in figure 3(c)–(f).

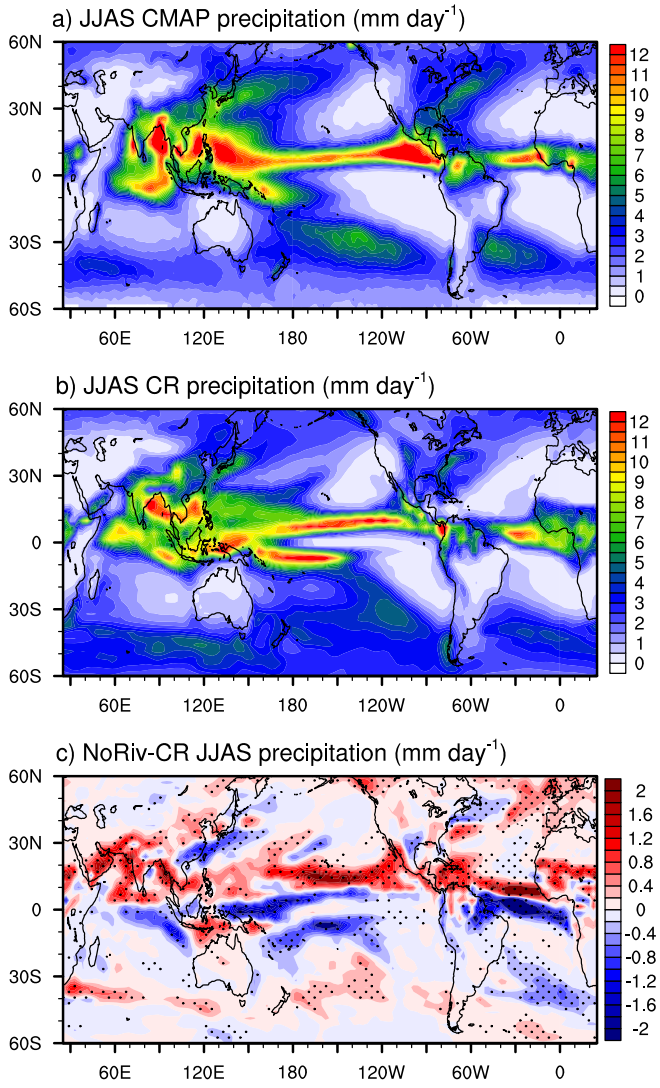

Figure 4. Monsoon simulation by CCSM3. Comparison of JJAS mean rainfall (mm day^{-1}) from (a) the Climate Prediction Center Merged Analysis of Precipitation (CMAP, Xie and Arkin 1996) and (b) the CR case. The model performs reasonably well in comparison with the observation. However, the maximum precipitation in the model is weaker compared to observations. (c) The mean difference between the two experiments (NoRiv–CR) in JJAS rainfall (mm day^{-1}). The differences are significant at 95% confidence level in the stippled region.

In the tropical Atlantic, a dipole SST pattern drives surface winds towards the warmer hemisphere, pushing the ITCZ farther north (Broccoli *et al* 2006). The associated cross-equatorial winds drive anomalous surface currents (figure 2(b)) which carry warm temperature anomalies to the northern Atlantic, increasing the SST (Huang and Mehta 2010). This is confirmed by the heat budget analysis (figure 3(e)) which shows that the meridional heat transport is much higher in the NoRiv case compared to that in the CR. As the SST increases, there is larger loss of heat from the ocean to the atmosphere (figure 3(c)) in NoRiv compared to CR. A similar mechanism is found to be responsible for generating warmer SST, when runoff is switched off, in the northern Pacific Ocean, albeit with magnitudes smaller compared to that in the Atlantic (figure 3(d), (f)). In contrast, the evolution of SST differences in the equatorial Pacific involves complex air–sea interaction. Cooler SST (in the NoRiv case) in the central Pacific generates a zonal pressure gradient that enhances equatorial easterlies which in turn enhances upwelling (see figure 7(a) for example), leading to the formation of a cold SST band along the equator.

SST changes do occur in a coupled ocean–atmosphere system, due to the evolving interaction between the ocean and atmosphere, in addition to changes in ocean mixing due to the weakening of upper layer stratification. Below we show that such interactions have the capability to alter the Indian summer monsoon and El Niño, which are two dominant features of the present–day climate in the tropics.

3.2. Impact on Indian summer monsoon

The mean monsoon rainfall simulated by the model agrees reasonably well with the CPC Merged Analysis

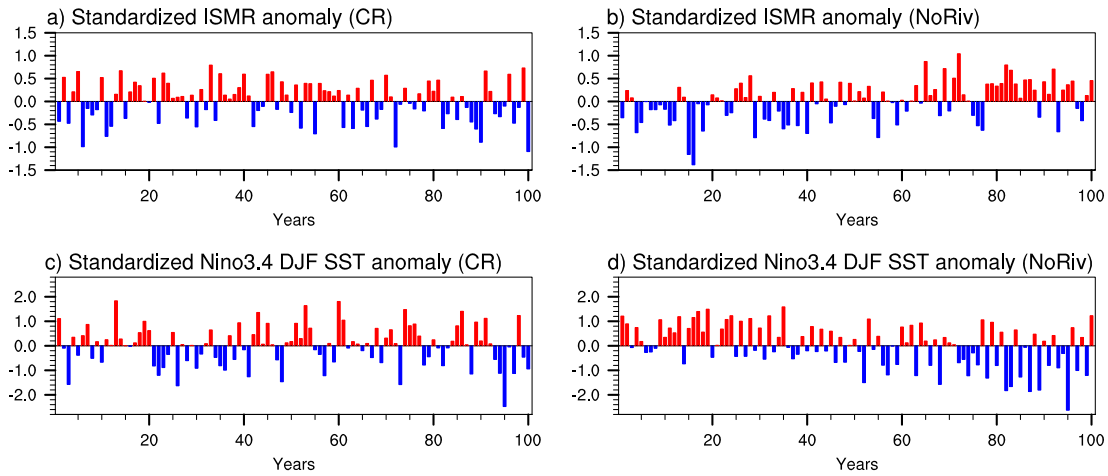

Figure 5. ISMR and El Niño in model simulations. Bar chart showing standardized anomaly of (a) control ISMR, (b) NoRiv ISMR, (c) control Niño3.4 DJF SST and (d) NoRiv Niño3.4 DJF SST. Since the model ISMR variability is low, we have used a criteria of half a SD to define a surplus, normal, or deficit year. For Niño3.4 index, anomalies greater than 1 are identified as El Niño and less than -1 are considered as La Niña events. Note that the number of surplus monsoon years and number of La Niña years are larger in the NoRiv case.

of Precipitation (CMAP) (Xie and Arkin 1996) data (figure 4(a), (b)). The summer monsoon rainfall over the Indian region has two maxima, one towards the mountains of Myanmar and the other seaward off the Sahyadris (Western Ghats). Both of these maxima are present in the model simulation albeit with slight differences in the location and values, owing to the limitations of models in reproducing the monsoon rainfall patterns accurately (Rajeevan and Nanjundiah 2009). A notable departure of the simulation compared to observations is the inability of the model to reproduce the high rain band in the western Pacific, off Philippines. The long term seasonal ISMR from rain gauges is 89 cm while the corresponding value from the CR simulation is 80 cm. The mean rainfall over India (8°N to 25°N, 70°E to 90°E) and its standard deviation from CR are 6.50 mm day^{-1} and 0.67 mm day^{-1}, respectively. Corresponding values from observations are 6.85 mm day^{-1} and 0.79 mm day^{-1} for the 1951–2003 period (Rajeevan *et al* 2006). Corresponding values for the NoRiv are 7.05 mm day^{-1} and 0.69 mm day^{-1}, respectively, in the last 50 years.

The major impact of runoff is expressed as a band of increasing rainfall that stretches from the northwestern part of India to the Bay of Bengal (figure 4(c)). A band of decreasing rainfall is also seen across the Indian Ocean between the equator and 15°S to the east of about 60°E extending upto the maritime continent. There is an increase of 0.74 mm day^{-1} in the western half of India (70°E to 80°E), while in the eastern half (80°E to 90°E), the rainfall increased by 0.25 mm day^{-1}.

In order to assess the interannual variability of monsoons, we have used a criteria of half a standard deviation to define a surplus or deficit year. The difference in actual rainfall between CR and NoRiv suggests that, after the initial oscillations, the absence of runoff causes a shift to a higher rainfall regime in the model (figure 6(a)). There are 25 flood and drought years each in the 100 year span of CR (figure 5(a)). In the NoRiv, in the first twenty years, the rainfall tends to be deficient and this tendency reduces drastically, and the occurrence of excess rainfall begins to be common after about the year 50 (figure 5(b)). In the first 50 years, there are 16 deficit and 6 excess monsoon years, while in the last 50 years of NoRiv, there are 17 strong flood years with only 7 deficit years (figure 5(b)). There is an apparent shift in the rainfall intensity from a weaker monsoon to a stronger monsoon in the latter half of NoRiv, especially in the last four decades (figure 5(b)). The mean difference (NoRiv–CR) in JJAS ISMR for the 60–100 year period of the model run is 8.6 cm. The mean seasonal rainfall for the same period in CR is 79 cm.

3.3. Impact on El Niño and its relationship to ISMR

The monsoon is a result of a rather complex interaction involving ocean, atmosphere and land. While the regularity of monsoons is nearly certain, its interannual variability is of major concern as the drought, normal and flood years are dependent on this variability. The shutting down of runoff resulted in slight summertime cooling in the Bay of Bengal, warming in the western equatorial Indian Ocean and cooling in the eastern equatorial Indian Ocean. These differences between CR and NoRiv, however, are far too small compared to that in the Pacific (figure 2(b). It is well known that the SST anomalies in the Pacific associated with El Niño and La Niña events have a major impact on the variability of the ISMR (Gadgil *et al* 2004).

El Niño affects the interannual variability of river discharge (Milliman and Farnsworth 2011, Dai *et al* 2009). We find that the converse is also true (figure 6(b)). The Niño3.4 index shows that the

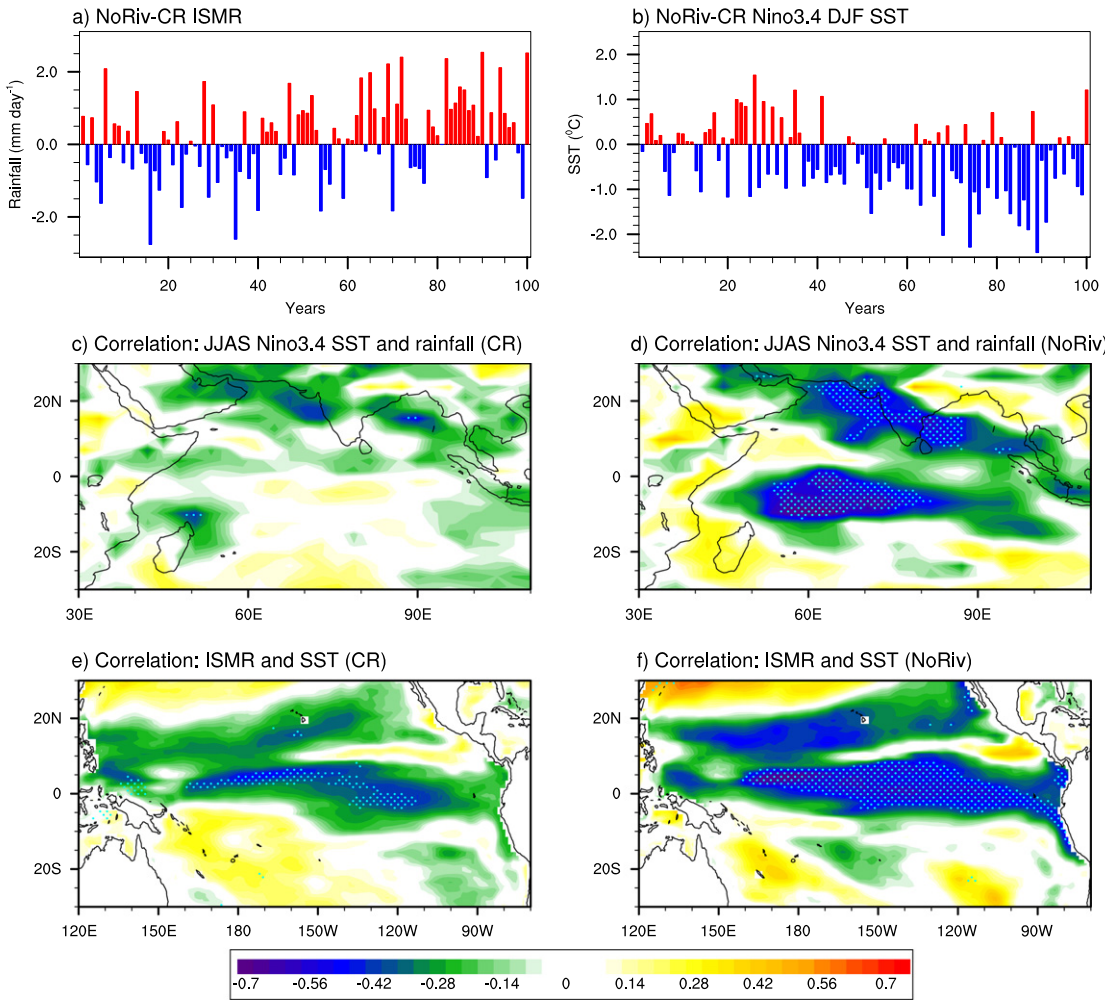

Figure 6. Impact of river runoff on monsoon and El Niño. (a) Difference (NoRiv–CR) in ISMR between model runs without and with river runoff. ISMR is defined as the mean rainfall (mm day^{-1}) for the region 8°N–25°N; 70°E–90°E for the months of JJAS. (b) Difference (NoRiv-CR) in Niño3.4 SST between model runs with and without river runoff. The Niño3.4 region is bounded by 120° W–170°W and 5°S–5°N. All differences are for the 50–100 year period of respective model runs. Correlation between Niño3.4 SST and rainfall from (c) the control run and (d) from the NoRiv. Correlation between ISMR and SST for (d) the control run and (e) for the NoRiv. The correlation shown in panels c to e are significant at 95% in the stippled region.

number of El Niño events is 7 and La Niña events is 6 in CR in the last 50 years of the model run, whereas the NoRiv produced 13 La Niña events and only 4 El Niño events (figure 5(c), (d)). The difference in Niño3.4 SST between NoRiv and CR clearly shows a shift towards a colder regime (figure 6(b)). Note that the spatial pattern of SST difference in the Pacific is not similar to a canonical La Niña which is characterized by cooling of a much larger region in the eastern Pacific. Nevertheless, a northward shift in the ITCZ seen in NoRiv (figure 4(c)), associated changes in wind-driven upwelling in the equatorial Pacific and a zonal gradient in SST (Bird *et al* 2014) are La Niña-like features. Futhermore, zonal section of the equatorial Pacific temperature shows a deepening of the thermocline to the west and shoaling to the east (figure 7(c)), nearly similar to the oceanic conditions during a La Niña episode (figure 7(d)). Shoaling of the thermocline in the eastern equatorial Pacific and the strengthening of east–west surface pressure gradient act as a feedback to the cooling (confined to 5°S–5°N) via wind–SST feedback mechanisms (Bjerknes 1969). Hence we refer to these events as 'La Niña–like' condition.

In order to examine the role of the Pacific Ocean SST anomalies on the ISMR, we have analysed the correlation between the ISMR and SST for both runs (figure 6(c, (d)). In CR, these two anomalies show weak negative correlation over most of India (figure 6(c)). On the other hand, when the river runoff into the ocean is switched off, this correlation (figure 6(d)) becomes remarkably stronger (~0.5), suggesting an increase in the influence of equatorial Pacific SST anomalies on the increasing summer rainfall over India.

La Niña-like cooling in the equatorial Pacific in the NoRiv modifies the large-scale circulation and precipitation patterns, including monsoon rainfall over India (Gadgil *et al* 2004). There is a dipole-like SST pattern in the Pacific and Atlantic, with warming in the northern tropical oceans and cooling at the

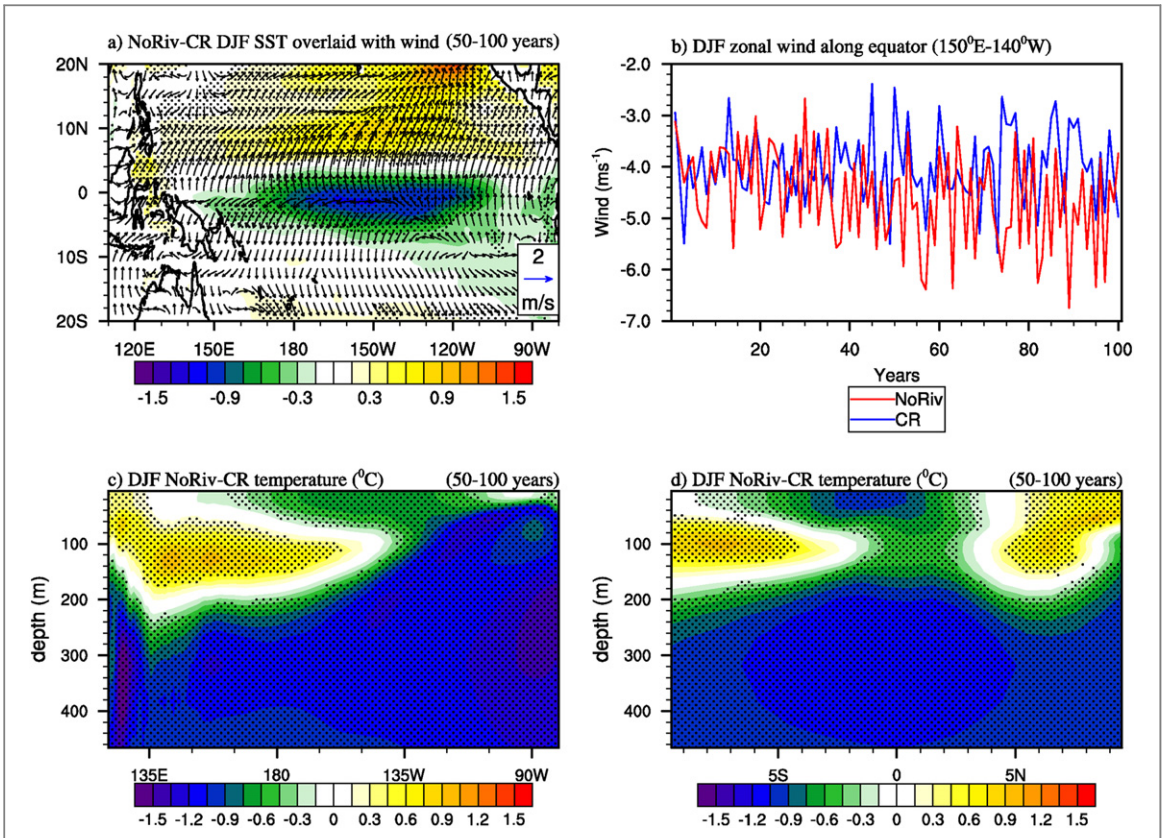

Figure 7. Figure showing the mechanism of cooling in the equatorial Pacific during DJF. (a) NoRiv–CR SST overlaid with winds, (b) zonal wind averaged over 150°E–140°W along the equator, (c) zonal section of temperature (averaged over 5°S–5°N) and (d) meridional section of temperature (averaged over 180°W–120°W).

equator and southern tropical oceans (figure 2(b)). This seesaw in SST across the equator shifts the ITCZ towards the warmer hemisphere (Broccoli *et al* 2006), along with a northward displacement of the thermal equator. The latitudinal position of the ITCZ modulates the large scale rainfall pattern across the hemispheres through changes in prevailing wind patterns (figure 7(a), (b)).

In CR, the ISMR has a strong negative correlation with the equatorial Pacific (figure 6(e)) suggesting the strong influence of ENSO on the ISMR. In NoRiv, this correlation has increased, covering a much larger region of the Pacific, in fact, extending all across the Pacific in two zonal bands (figure 6(f)). In NoRiv, the strong negative correlation band is found to spread across the entire Pacific, with maximum correlated regions shifted slightly northward of the equator (figure 6(f)). The strength of the teleconnection depends on the location of the SST anomaly in the equatorial Pacific (Ashok *et al* 2007) which suggests that as the cold SST band extends westward in NoRiv, the teleconnection with the monsoon strengthens (Kumar *et al* 2006, Ashok *et al* 2001).

4. Discussion and conclusions

The linkage between SST changes in the equatorial Pacific and the ISMR can be understood in terms of existing theories of teleconnections through the mid-latitudes. Shaman and Tziperman 2007 (henceforth ST2007) proposed that the changes in summertime central Pacific SST during El Niño and La Niña cause convective anomalies (positive anomalies during an El Niño and negative during a La Niña) in the ITCZ of the equatorial Pacific. ST2007 further showed that such positive (negative) convective anomalies lead to divergence (convergence) and westward propagating vorticity anomalies along the North African–Asian jet (NAA, this is a jet that extends from Africa to the Pacific Ocean above the Asian land mass (figure 8(b))). The vorticity anomalies are negative during a cooling event and positive during a warming event. Negative vorticity anomalies (related to cooling in the central equatorial Pacific) lead to warm temperature anomalies in the upper troposphere over the Asian land mass, that strengthens the meridional temperature gradient between the Asian landmass and the equatorial Indian Ocean. This increases intraseasonal activity over the Indian region which leads to a stronger summer monsoon (Jiang *et al* 2004). Our simulations suggest that the absence of river runoff leads to a cooler equatorial Pacific and a consequent strengthening of meridional temperature gradients (figure 8(a)) through changes in upper level vorticity (figure 8(b)), as described above. In addition, the absence of river runoff causes an increase in the

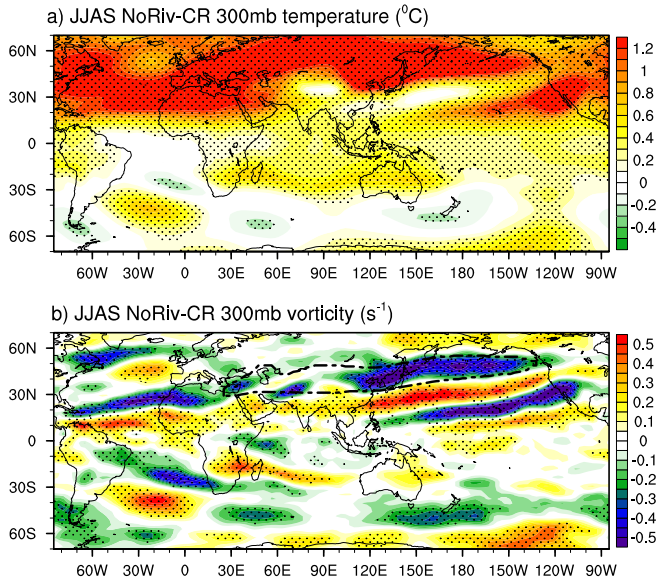

Figure 8. Maps of difference (NoRiv–CR) in (a) 300 mb temperature (°C) field averaged for the months of June–September (JJAS) and (b) 300 mb vorticity for JJAS. Both differences are plotted for the 50–100 year of the model runs. The dashed contour in panel (b) shows the climatological axis of the North African–Asian Jet, chosen as the zonal wind contour of 17 m s^{-1} at 300 mb, from the climatology of CR for JJAS.

meridional gradient of the upper tropospheric temperature over the Asian region which in turn results in an increase in the vertical shear of zonal wind through changes in thermal wind balance (ST2007).

The impact of river runoff into the ocean on climate is a little known facet of the climate system. In this study, results from a pair of 100 year simulations using CCSM3 have been presented, one including river runoff and the other excluding it. In the absence of river runoff, the ocean salinity increases everywhere and global mean SST increases by about 0.5°C. The ISMR increases, along with an increase in the number of La Niña events in the Pacific and the correlation between ISMR and the Pacific Ocean SST anomalies strengthens in the absence of river runoff. The changes in SST include cooling of the central equatorial Pacific. This alters Rossby wave propagation in the NAA Jet axis. The altered Rossby wave propagations causes warming in the upper troposphere over the Asian land mass. This leads to strengthening of the upper tropospheric meridional temperature gradient. This in turn strengthens the Indian monsoon and provides a link between ISMR and the Pacific Ocean (as shown by ST2007).

An interesting feature that has emerged from our analysis is the large response of the Pacific SST despite the smaller quantity of runoff it receives compared to that of the Atlantic and Indian Ocean relative to the total surface area (Dai and Trenberth 2002, Milliman and Farnsworth 2011). Mechanisms that lead to large SST changes in the Pacific and their spatial inhomogeneity require further analysis. An unresolved issue is the contribution from individual river systems. Considering that several river basins of the world are projected to face serious water stress in the future climate, the role of individual river basins on climate could be non-negligible.

We conclude that river runoff into the oceans has considerable impact on components of the present climate that affect billions of people, and call for a detailed understanding of this lesser known facet of our climate. This requires rather accurate quantification of river runoff into the oceans and assessment of its impact on climate, at both short and long time scales, using models. The need for such an effort is reinforced by both scientific curiosity and societal needs. Since its discovery in the Western Equatorial Pacific Ocean in the early nineties (Lukas and Lindstorm 1991), evidence has been accumulating from several parts of the world's oceans of salinity effects on the mixed layer depth as well as SST to a level that is pertinent to intensify disastrous weather events (Balaguru *et al* 2012). We have shown that salinity and SST anomalies generated by river runoff are significant, particularly over regions that have a high potential for positive feedback in largescale air–sea interaction. There is a possible amplification of this effect in the future as growing population escalates water stress, and there is increasing demand for fresh water for drinking and irrigation (Vorosmarty *et al* 2010, Immerzeel *et al* 2010) that forces nations to reduce the quantum of release of river water into the oceans (Grumbine and Pandit 2013). Since there is a significant impact of river runoff into the oceans even in regions far away from the sources, further modeling experiments are likely to provide the most immediate means for assessing the responses.

Acknowledgments

This study was partly funded by the Indian Ocean Modeling (INDOMOD) programme of Indian National Centre for Ocean Information Services (INCOIS) and the CTCZ program funded by the Ministry of Earth Sci., Govt. of India. Thanks to NCAR for providing the CCSM3.0 code and data files. Thanks to FIST, Dept. Sci & Tech., Govt. of India and Divecha Centre for Climate Change for funding the HPC system at CAOS. Thanks to S Sukumaran for his assistance with setting–up CCSM. We thank two anonymous reviewers for their comments and suggestions which improved the clarity of the paper.

References

Ashok K, Behera S K, Rao S A, Weng H and Yamagata T 2007 El Niño Modoki and its possible teleconnection *J. Geophys. Res.* **112** C11007

Ashok K, Guan Z and Yamagata T 2001 Impact of the Indian Ocean dipole on the relationship between the Indian monsoon rainfall and ENSO *Geophysical Research Letters* **28** 4499–502

Balaguru K, Chang P, Saravanan R, Leunga L R, Xu Z, Li M and Hsieh J S 2012 Ocean barrier layer's effect on tropical cyclone intensification *Proc. Natl Acad. Sci. USA* **109** 14343–7

Beven K J and Kirkby M J 1979 A physically based variable contributing area model of basin hydrology *Hydrological Sciences Bulletin* **24** 43–69

Bird B W, Polisar P J, Leic Y, Thompson L G, Yaoc T, Finneye B P, Bain D J, Pompeani D P and Steinman B A 2014 A Tibetan lake sediment record of Holocene Indian summer monsoon variability *Earth and Planetary Science Letters* **399** 92–102

Bjerknes J 1969 Atmospheric teleconnections from the equatorial Pacific *Mon. Weather Rev.* **97** 163–72

Branstetter M L 2001 Development of a parallel river transport algorithm and applications to climate studies *Ph.D. dissertation* University of Texas at Austin

Briegleb B P, Bitz C M, Hunke E C, Lipscomb W H, Holland M M, Schramm J L and Moritz R E 2004 Scientific description of the sea ice component of the Community Climate System Model, Version 3. Tech. Rep. NCAR/TN- 463+STR *National Center for Atmospheric Research, Boulder* 78

Broccoli A J, Dahl K A and Stouffer R J 2006 Response of the ITCZ to northern hemisphere cooling *Geophys. Res. Lett.* **33** L01702

Collins W D *et al* 2006a The community climate system model version 3 (CCSM3) *J. Clim.* **19** 2122–43

Collins W D, Rasch P J, Boville B A, Hack J J, McCaa D L, Williamson D L, Briegleb C M, Bitz S J, Lin S J and Zhang M 2006 The formulation and atmospheric simulation of the community atmosphere model: CAM3 *J. Clim.* **19** 2144–61

Dai A, Qian T and Trenberth K E 2009 Changes in continental freshwater discharge from 1948 to 2004 *J. Clim.* **22** 2773–92

Dai A and Trenberth K 2002 Estimates of freshwater discharge from continents: latitudinal and seasonal variations *Journal of Hydrometeorology* **3** 660–87

de Boyer Montegut C, Mignot J, Lazar A and Cravatte S 2007 Control of salinity on the mixed layer depth in the world ocean: 1. General description *J. Geophys. Res.* **112** C06011

Dickinson R E, Oleson K W, Bonan G, Hoffman F, Thornton P, Vertenstein M, Yang Z L and Zeng X 2006 The Community Land Model and its climate statistics as a component of the Community Climate System Model *J. Clim.* **19** 2302–24

Durack P J, Wijffels S E and Matear R J 2012 Ocean salinities reveal strong global water cycle intensification during 1950 to 2000 *Science* **336** 455–8

Fedorov A V, Pacanowski R, Philander S G and Boccaletti G 2004 The effect of salinity on the wind-driven circulation and the thermal structure of the upper ocean *J. Phys. Oceanogr.* **34** 1949–66

Gadgil S, Vinayachandran P N, Francis P A and Gadgil S 2004 Extremes of Indian summer monsoon rainfall, ENSO, Equatorial Indian Ocean Oscillation *Geophys. Res. Lett.* **31** L12213

Grumbine R E and Pandit M K 2013 Threats from India's Himalaya dams *Science* **339** 36–37

Huang B and Mehta V M 2010 Influences of freshwater from major rivers on global ocean circulation and temperatures in the MIT ocean general circulation model *Advances in Atmospheric Sciences* **27** 455–68

Immerzeel W W, van Beek L P H and Bierkens M F P 2010 Climate change will affect the Asian water towers *Science* **328** 1382–85

Jiang X, Li T and Wang B 2004 Structures and mechanisms of the northward propagating boreal summer intraseasonal oscillation *J. Clim.* **17** 1022–39

Kumar K K, Rajagopalan B, Bates M H B and Cane M 2006 Unraveling the mystery of Indian Monsoon failure during El Niño *Science* **314** 114–9

Lagerloef G S E 2002 Introduction to the special section: The role of surface salinity on upper ocean dynamics, air-sea interaction and climate *J. Geophys. Res.* **107** 8000

Lukas R and Lindstorm E 1991 The mixed layer of the western equatorial Pacific Ocean *J. Geophys. Res.* **96** 343–57

Milliman J D and Farnsworth K L 2011 *River Discharge to the Coastal Ocean: A Global Synthesis* 1st edn (Cambridge, UK: Cambridge University Press)

Rajeevan M, Bhate J, Kale J D and Lal B 2006 High resolution daily gridded rainfall data for the Indian region: Analysis of break and active monsoon spells *Curr. Sci.* **91** 296–306

Rajeevan M and Nanjundiah R S 2009 Coupled model simulations of the twentieth century climate of the Indian Monsoon *Current Trends in Science: Platinum Jubilee Special, Indian Academy of Sciences* 537–57

Rao R R and Sivakumar R 2003 Seasonal variability of sea surface salinity and salt budget of the mixed layer of the north Indian Ocean *Journal of Geophysical Research* **108** 3009

Seager R, Naik N and Vecchi G A 2010 Thermodynamic and dynamic mechanisms for large-scale changes in the hydrological cycle in response to global warming *J. Clim.* **23** 4651–68

Seidov D and Haupt B J 2003 On sensitivity of ocean circulation to sea surface salinity *Glob. Planet. Change* **36** 99–116

Seo H, Xie S P, Murtugudde R, Jochum M and Miller A J 2009 Seasonal effects of Indian Ocean freshwater forcing in a regional coupled model *J. Clim.* **22** 6577–96

Shaman J and Tziperman E 2007 Summer-time ENSO-North African-Asian Jet teleconnection and implications for the Indian monsoons *Geophysical Research Letters* **34** L11702

Shankar D, Vinayachandran P N and Unnikrishnan A S 2002 The monsoon currents in the north Indian Ocean *Prog. Oceanogr.* **52** 63–120

Smith R D and Gent P R 2002 Reference manual for the Parallel Ocean Program (POP), ocean component of the Community Climate System Model (CCSM2.0 and 3.0) *Los Alamos National Laboratory Technical Report* LA-UR-02-2484.

Trenberth K E, Smith L, Qian T, Dai A and Fasullo J 2007 Estimates of the global water budget and its annual cycle using observational and model data *J. Hydrometeorol.* **8** 758–69

Vinayachandran P N and Nanjundiah R S 2009 Indian Ocean sea surface salinity variations in a coupled model *Clim. Dyn.* **33** 245–63

Vorosmarty C J *et al* 2010 Global threats to human water security and river biodiversity *Nature* **467** 555–61

Williams P D, Guilyardi E, Madec G, Gualdi S and Scoccimarro E 2010 The role of mean ocean salinity in climate *Dynamics of Atmospheres and Oceans* **49** 108–23

Xie P and Arkin P A 1996 Global precipitation: a 17-year monthly analysis based on gauge observations, satellite estimates, and numerical model outputs *Bull. Am. Meteorol. Soc.* **78** 2539–58

Zhang L and Wu L 2012 Can oceanic freshwater flux amplify global warming? *J. Clim.* **25** 3417–30